Phase-stepping technique for highly sensitive microscopic surface plasmon resonance biosensor

Chonglei Zhang,[1] Rong Wang,[1] Yijia Wang,[2] Siwei Zhu,[2] Changjun Min,[1,4] and X.-C. Yuan[3,5]

[1]Institute of Modern Optics, Key Laboratory of Optical Information Science & Technology, Ministry of Education of China, Nankai University, Tianjin 300071, China

[2]Nankai University Affiliated Hospital, Tianjin 300121, China

[3]Institute of Micro & Nano Optics, College of Optoelectronic Engineering, Shenzhen University, Shenzhen 518060, China

[4]e-mail: cjmin@nankai.edu.cn

[5]e-mail: xcyuan@szu.edu.cn

Received 7 October 2013; revised 26 December 2013; accepted 28 December 2013; posted 3 January 2014 (Doc. ID 199061); published 5 February 2014

In this paper, the phase-stepping technique is applied to improve a phase-sensitive surface plasmon resonance biosensor based on differential interferometry between focused radially polarized and azimuthally polarized cylindrical vector beams. Detailed analysis is presented for the phase-stepping method, and the least squares unwrapping algorithm is employed to detect the phase distribution in correspondence to the refractive index of sample. Benefiting from the phase-stepping technique, both the measurement speed and sensitivity are improved significantly. The proposed sensor maintains high sensitivity of 9.4×10^{-7} RIU/1° and a wide dynamic range of 0.35 RIU simultaneously. Furthermore, the real-time binding reaction process of bovine serum albumin with antibody is monitored to verify the system for potential biological applications.

OCIS codes: (120.3180) Interferometry; (170.3890) Medical optics instrumentation; (240.6680) Surface plasmons; (280.4788) Optical sensing and sensors; (100.5088) Phase unwrapping.

http://dx.doi.org/10.1364/AO.53.000836

Surface plasmon resonance (SPR) has drawn much attention because it is highly sensitive to perturbations in the surrounding medium, consequently making SPR significant for a host of optical sensing applications [1,2]. Over the past two decades, SPR biosensors have widely been employed for detection of assays in basic biological, materials science, pharmaceutical products, clinical diagnostics, environmental, and agricultural sampling kits [3].

Among four different detecting mechanisms of SPR biosensors based on intensity, angle, spectrum, and phase, respectively, the phase-sensitive biosensors usually provide the highest phase sensitivity due to a much more intense probing electric field in the region of maximal phase variation compared with that of the amplitude change and much lower level of phase noises compared to amplitude noises [4,5]. With the help of the interferometric technique, which is extremely popular for optical phase detection [6,7], the sensitivity limit of phase-sensitive SPR biosensors was further improved, and thus resolution of 10^{-8} RIU or better had experimentally

1559-128X/14/050836-05$15.00/0

been achieved in phase-sensitive SPR biosensors [8–13]. However, the dynamic range of these SPR biosensors is only around the order of 10^{-3}–10^{-4} RIU, which is too narrow and strongly limits their practical applications [1]. To improve an SPR sensor with both high sensitivity and wide dynamic range, several techniques have been demonstrated, such as photo-elastic modulate [14] and cylindrical lens [13]. Recently we reported a new phase-sensitive SPR biosensor with both high sensitivity and wide dynamic range, based on differential phase measurement between radially polarized (RP) and azimuthally polarized (AP) cylindrical vector beams in a high numerical aperture (NA) objective-focusing configuration [15]. In this paper, we apply the phase-stepping and phase-unwrapping techniques to refine and further improve the phase detection of the SPR sensing system. Compared with the sinusoidal curve fitting method to extract phase in fringe analysis reported in our earlier work [16], the phase-stepping method not only increases the measurement speed but also improves the measurement sensitivity. Combining an angular mechanism with phase detection, the proposed biosensor system maintains the unique advantages in terms of both high sensitivity of 9.4×10^{-7} RIU/1° and wide dynamic range of 0.35 RIU at the same time.

A schematic of the experimental setup of our SPR biosensor system is shown in Fig. 1. The excitation source is a linearly polarized He–Ne laser at the wavelength of 633 nm, converted to circularly polarized light with a $\lambda/4$ wave plate. Then an AP beam is generated with the wave-train suppression technique applying a microfabricated spiral phase plate and an azimuthal-type analyzer (AA) [17]. Two half-wave plates are used to convert the generated AP beam into a mixed RP and AP beam with an included angled of $3\pi/8$ [15]. It follows that a Michelson interferometer is incorporated in the system to perform differential phase measurement between RP and AP beams. The signal beam of interferometer is tightly focused onto the glass-gold interface by an oil immersion objective lens with an NA of 1.49. A 45 nm (±2 nm) gold film, which is well optimized to provide a sharp phase jump, is deposited onto the glass substrate. In the reference arm, however, the beam directly incidents on a silver mirror mounted on the end of a piezoelectric transducer (PZT). We control the accurate position of the PZT with step of 79 nm (about $\lambda/8$). In the output path, a polarization analyzer, which consists of the beam splitter, AAs, and the polarization rotator, is used to separate the exit beam into RP and AP light. Two synchronized CCDs (1280 × 960, Point Grey Research, Flea 2) are used to capture the signals of RP and AP light. Digitalized intensity data are then processed in a personal computer to deliver the differential phase information with a fringe-analysis and phase-extraction program.

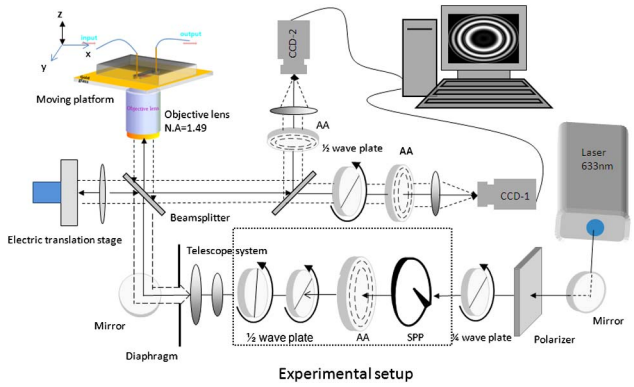

Fig. 1. Experimental setup for measuring the differential phase between RP and AP beams in an inverted microscope configuration.

In the proposed high NA focusing configuration, RP and AP beams are rotational symmetric transverse magnetic (TM) and transverse electric (TE) polarized with respect to the surface, respectively. Because of the coupling of the focused RP component (TM) to surface plasmon (SP) mode at the typical resonance angle, a dark ring formed at the back focal plane is captured by the CCD, as shown in Fig. 2(a), where the ratio of the dark ring to the outside boundary corresponds to the sample's refractive index. A related study has shown that the near-field distribution of the excited SP on the dielectric-metal interface takes the form of an evanescent Bessel beam, with a full-width half-maximum of 0.343λ for central peak [18]. The three-dimensional electric field distribution of SP is calculated with the Richards and Wolf theory [19,18], as shown in Fig. 2(b). The central peak can be used to detect the refractive index information of the sample and also to noninvasively probe the structure and to examine the dynamics around the contact regions of cells. These cell-substrate contact regions are of significant interests in cell biology, such as understanding of the mechanisms for cell motility and the structural organization of cell surface receptors in response to external signals [20]. Although the shift of dark ring can be utilized to detect the change of the

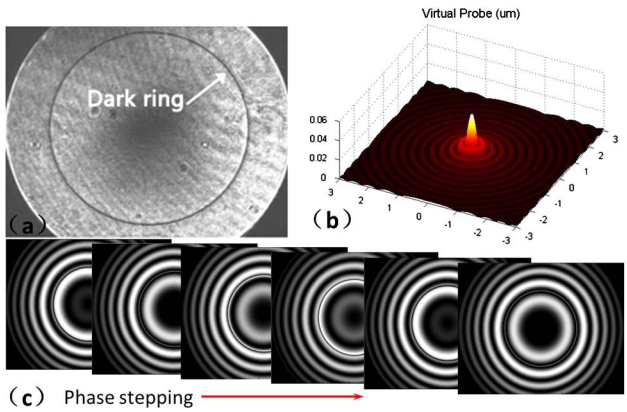

Fig. 2. (a) Image captured on the CCD. The inner dark ring corresponds to the SPR excitation. (b) RP beam focused on a planar metallic surface enable an evanescent Bessel SP wave. (c) Get six different interferometry images through phase stepping method.

sample's refractive index this detection is limited by the pixel size and number of CCD. When the change of the sample's refractive index is smaller than 10^{-4} RIU, the shift of the dark ring is smaller than one pixel; hence the slight change of refractive index could not be distinguished in CCD. In contrast, based on the phase detection technique, even the shift of the dark ring is smaller than one pixel; the phase change can be detected to measure the slight change of refractive indices. So we can use the interferometry method to obtain the interferograms [such as Fig. 2(c)] by adjusting the distance between the microscopic objective and the gold film to get a fixed number of fringes for refractive index detection. This method could also increase the signal-to-noise ratio (SNR) because the proper algorithms are chosen.

Here, the temporal phase stepping method is introduced to detect the phase change. Compared with the sinusoidal curve fitting method reported in our earlier work [11], the phase-stepping technique not only increases the measurement speed but also improves the measurement sensitivity. Different steps of the phase-stepping method are compared; the six-step phase stepping method can effectively reduce the linearity error, quadratic error of the PZT, and the second error of the detector [21,22]. In this method, six frames of the interferogram are recorded sequentially when the phase of reference beam shifts by a step of $\pi/2$ between every two successive frames, as shown in Fig. 2(c). While the dark ring position is not changed, only the PZT modulated phase changes accompany with the stripe moving. Then the initial phase distribution $\varphi(x,y)$ in interferogram is calculated from the intensity distributions of six phase stepping interferograms with the following formula [23]:

$$\varphi(x,y) = \operatorname{atan}\frac{-3I_1 + 4I_3 - I_5}{I_0 - 4I_2 + 3I_4}, \tag{1}$$

where $I_0 - I_5$ denote the intensity distribution of the six phase-stepping interferograms sequentially. The phase distribution acquired directly from Eq. (1) is wrapped in the range of $(-\pi \sim \pi)$. To restore the detected phase beyond the range, the phase-unwrapping algorithm is essentially employed in the data process. Here, the least squares method is used to unwrap the phase. We find that it is robust in terms of SNR and the minimum difference between the original phase and the final phase with reenvelope is guaranteed [24].

The interferogram of RP and AP beams is captured with two synchronized CCDs (as shown in Fig. 1). With six-step displacement of PZT, six successive images are recorded independently to detect the phase distribution, as shown in Figs. 3(a) and 3(b). The obvious difference between them appears in the dark ring position where the phase jump occurs corresponding to the resonance angle of SP. The overall phase distribution is relatively flat except for edge burrs caused by noise. With the measurement of

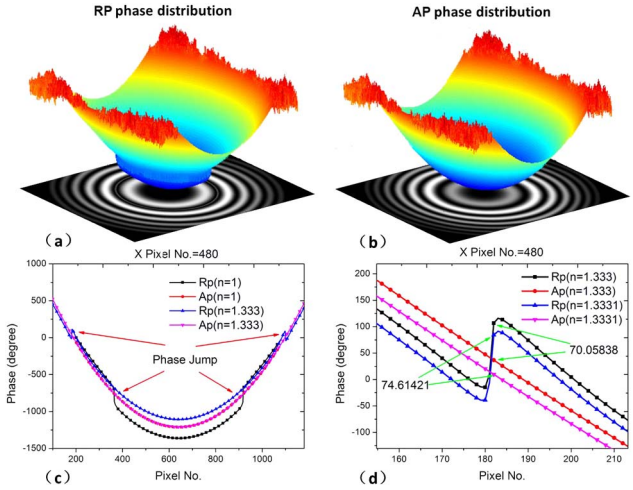

Fig. 3. Phase distributions of (a) RP interferogram and (b) AP interferogram. The sample is air. The bottom grayscale figure is the interferogram and the top colorful figure is the corresponding phase distribution. (c) Phase distributions of RP and AP at a line across the center of interferogram; the refractive index of sample is $n = 1$, 1.333 RIU. Phase jump occurs in the position of dark ring. (d) Phase distributions of RP and AP around the phase jump (dark ring) region; the refractive index of sample is $n = 1.333$, 1.3331 RIU.

phase difference between RP and AP, environmental disturbance is eliminated and hence greatly improves the accuracy of phase measurement for sensing. When two samples have great difference in refractive indices, for example $n_1 = 1$ RIU and $n_2 = 1.333$ RIU, as shown in Fig. 3(c), the position of phase jump locates in two distant pixels in CCD image; thus a wide dynamic range for measuring refractive index can be obtained according to the phase jump at different pixels. When two samples have a tiny difference in refractive indices, for example, $n_1 = 1.333$ RIU and $n_3 = 1.3331$ RIU as shown in Fig. 3(d), the position of phase jump locates in the same pixel but with a variation of phase jump value; thus their slight difference in refractive indices can be measured by different phase jump values at the same pixel. As a result, with a 1.49 NA focusing objective lens, we can achieve either a wide-range measurement of refractive indices from 1 to 1.35 RIU at different pixels in CCD or a more exact detection in a small range of approximately 0.0012 RIU at single pixel.

To verify the improved performance of the proposed sensor, we measure a series of different concentrations of alcohol and water mixed solutions, ranging from 0.015% (1.333009 RIU) to 0.24% (1.333132 RIU) with a small increment of 0.015% (0.000009 RIU). Sample fluids with three different concentrations are simultaneously drived with the Syringe Pump (BASi, MD-1001) that enables smooth and constant flow at precisely controlled rates ranging from 0.001 to 500 μL/ min. The injection of sample fluids into the microchannel is controlled with a syringe selector (BASi, MD-1508), able to quickly toggle one syringe to the next without interrupting flow

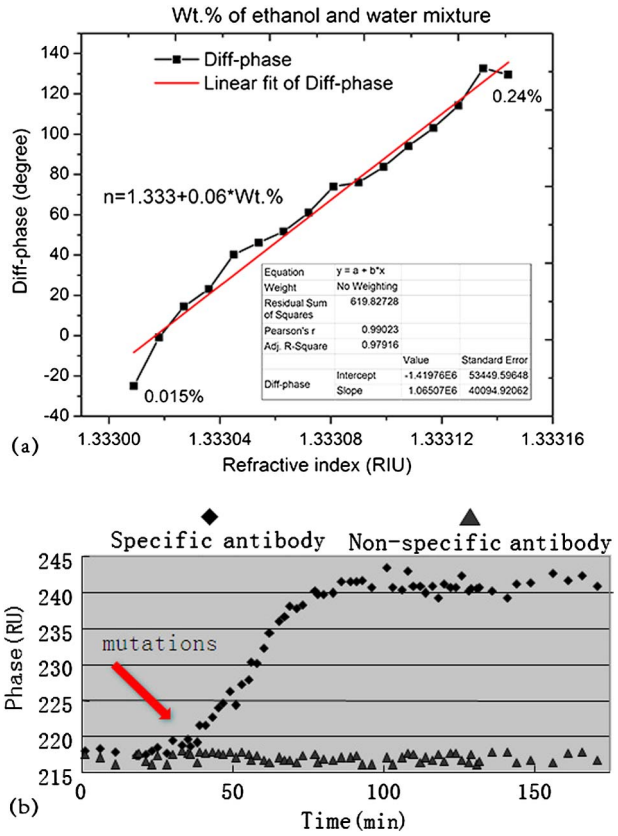

Fig. 4. (a) Differential phase measurements versus refractive index of different solutions mixed of alcohol and water. (b) Real-time measure of the process of bovine serum albumin (BSA) binding reaction with antibody by phase detection.

or introducing air bubbles into the system. Such a controlling system of flows eliminated the pressure change that results from the short stop of the syringe when changing the solution as well. During the experiment, the CCD is operated in the mode of 16 bits to improve the angular resolution. The active thermostating elements with minimum accuracy up to 0.01° controlled by PID mode is also adopted to tackle with the temperature drift problems. The measured result is shown in Fig. 4(a), where each data point is obtained by averaging three consecutive measurements with high stability in the time domain, based on only average the left-most and the right-most points distributed symmetrically on along the dark ring in a single measurement, and we also linearly fit the experiment data. The sensitivity of the proposed sensor is obtained as 9.4×10^{-7} RIU/1° due to the sensitivity being the inverse of the slope of linear fit of diff-phase, and if we get a higher phase resolution, the ultimate sensitivity limit would be lower. In Fig. 4(b), due to fast measurement speed, we are able to carry out real-time study of binding reaction process of bovine serum albumin (BSA) with antibody, where the BSA is firstly covered on the surface of gold film as antigen. Then the EGF antibody (non-specific antibody) or BSA antibody (specific antibody) with a concentration of 0.1 μg/ml is injected into the micro-cell at a speed of 100 μl/ min. We have clearly observed that the specific antibodies reaction with BSA in a slow-rise process and finally get a plate. The rise time is about 50 min to achieve the overall phase shift of about 25°, indicating a specific antibody binding with the BSA. The detection sensitivity of the system can be further improved with optimized thickness of metal films, more stable mechanical structure, and appropriate temperature controlling system in future.

1. Conclusion

In this paper, we applied the phase-stepping technique to improve a microscopic configuration based differential phase measurement SPR biosensor between radially and AP beams. A six-step phase-shifting method is utilized to extract accurate phase change with an optimized phase unwrapping algorithm. Compared with the previous sinusoidal curve fitting method, the phase-stepping technique increases both the measurement speed and sensitivity. The feasibility of the system is fully verified through measuring different proportions of alcohol and water mixture and real-time monitoring of BSA and antibody reaction process. The proposed system combines angular mechanism with phase detection, maintaining both high sensitivity of 9.4×10^{-7}RIU/1° and a wide dynamic of 0.35 RIU simultaneously.

This work was partially supported by the National Nature Science Foundation of China under Grant Nos. 61036013, 61138003, and 61377052. X. C. Y. acknowledges the support given by the Ministry of Science and Technology of China under grant No. 2009DFA52300 and Tianjin Municipal Science and Technology Commission under Grant No. 11JCZDJC15200. C.J.M. acknowledges the support provided by Nature Science Foundation of China under Grant No. 11204141 and the Tianjin Municipal Science and the support provided by Technology Commission under Grant No. 12JCYBJC31000.

References

1. J. Homola, S. S. Yee, and G. Gauglitz, "Surface plasmon resonance sensors: Review," Sens. Actuators B **54**, 3–15 (1999).
2. J. Homola, "Present and future of surface plasmon resonance biosensors," Anal. Bioanal. Chem. **377**, 528–539 (2003).
3. R. L. Rich and D. G. Myszka, "Survey of the year 2005 commercial optical biosensor literature," J. Mol. Recogn. **19**, 478–534 (2006).
4. Y. H. Huang, H. P. Ho, S. K. Kong, and A. V. Kabashin, "Phase-sensitive surface plasmon resonance biosensors: methodology, instrumentation and applications," Ann. Phys. **524**, 637–662 (2012).
5. A. V. Kabashin, S. Patskovsky, and A. N. Grigorenko, "Phase and amplitude sensitivities in surface plamson resonance bio and chemical sensing," Opt. Express **17**, 21191–21204 (2009).
6. S. P. Ng, C. M. L. Wu, S. Y. Wu, H. P. Ho, and S. K. Kong, "Differential spectral phase interferometry for wide dynamic range surface plasmon resonance biosensing," Biosens. Bioelectron. **26**, 1593–1598 (2010).
7. A. V. Kabshin and P. I. Nikitin, "Surface plasmon resonance interferometer for bio- and chemical-sensors," Opt. Commun. **150**, 5–8 (1998).
8. A. V. Kabashin, V. E. Kochergin, and P. I. Nikitin, "Surface plasmon resonance bio- and chemical sensors with phase-polarization contrast," Sens. Actuators B **54**, 51–56 (1999).

9. H. P. Ho, W. W. Lam, and S. Y. Wu, "Surface plasmon resonance sensor based on the measurement of differential phase," Rev. Sci. Instrum. **73**, 3534–3539 (2002).
10. H. P. Ho and W. W. Lam, "Application of differential phase measurement technique to surface plasmon resonance sensors," Sens. Actuators B **96**, 554–559 (2003).
11. Y. C. Li, Y. F. Chang, L. C. Su, and C. Chou, "Differential-phase surface plasmon resonance biosensor," Anal. Chem. **80**, 5590–5595 (2008).
12. H. P. Chiang, J. L. Lin, and Z. W. Chen, "Highly sensitivity surface plasmon resonance sensor based on phase interrogation at optimal incident wavelengths," Appl. Phys. Lett. **88**, 141105 (2006).
13. Y. H. Huang, H. P. Ho, S. Y. Wu, S. K. Kong, W. W. Wong, and P. Shum, "Phase sensitive SPR sensor for wide dynamic range detection," Opt. Lett. **36**, 4092–4094 (2011).
14. P. P. Markowicz, W. C. Law, A. Baev, P. N. Prasad, S. Patskovsky, and A. V. Kabashin, "Phase-sensitive time-modulated surface plasmon resonance polarimetry for wide dynamic range biosensing," Opt. Express **15**, 1745–1754 (2007).
15. R. Wang, C. Zhang, Y. Yang, S. Zhu, and X.-C. Yuan, "Focused cylindrical vector beam assisted microscopic pSPR biosensor with an ultrawide dynamic range," Opt. Lett. **37**, 2091–2093 (2012).
16. C. Zhang, R. Wang, C. Min, S. Zhu, and X.-C. Yuan, "Experimental approach to the microscopic phase-sensitive surface plasmon resonance biosensor," Appl. Phys. Lett. **102**, 011114 (2013).
17. K. J. Moh, X.-C. Yuan, J. Bu, R. E. Burge, and B. Z. Gao, "Generating radial or azimuthal polarization by axial sampling of circularly polarized vortex beams," Appl. Opt. **46**, 7544–7551 (2007).
18. Q. Zhan, "Evanescent Bessel beam generation via surface plasmon resonance excitation by a radially polarized beam," Opt. Lett. **31**, 1726–1728 (2006).
19. B. Richards and E. Wolf, "Electromagnetic diffraction in optical systems. II. Structure of the image field in an aplanatic system," Proc. R. Soc. Lond. Math. Phys. Sci. **253**, 358–379 (1959).
20. D. Axelrod, "Cell-substrate contacts illuminated by total internal reflection fluorescence," J. Cell Biol. **89**, 141–145 (1981).
21. B. Zhao, "A statistical method for fringe intensity-correlated error in phase-shifting measurement: the effect of quantization error on the N-bucket algorithm," Meas. Sci. Technol. **8**, 147–153 (1997).
22. J. V. Wingerden, H. J. Frankena, and C. Smorenburg, "Linear approximation for measurement errors in phase shifting interferometry," Appl. Opt. **30**, 2718–2729 (1991).
23. K. Qian, "Comparison of some phase-shifting algorithms with a phase step of Π/2," Proc. SPIE **4596**, 310–313 (2001).
24. D. C. Ghiglia and L. A. Romero, "Robust two-dimensional weighted and unweighted phase unwrapping that uses fast transforms and iterative methods," J. Opt. Soc. Am. **11**, 107–117 (1994).